JOURNAL OF MATERIALS SCIENCE 22 (1987) 839–852

Thermally activated martensite in copper alloys

P. J. MOROZ*, R. TAGGART, D. H. POLONIS‡
Department of Mechanical Engineering and ‡Department of Materials Science and Engineering, University of Washington, Seattle, Washington 98195, USA

The mechanisms of the thermally induced fcc–hcp transformation in Cu–Ge alloys have been investigated by hot-stage microscopy and TEM techniques. The growth and thickening processes for the transformation are best described in terms of isothermal martensite growth in which the hcp phase formation is controlled by the rapid propagation of fine platelets having thicknesses ranging from 5 to 30 nm. The transformation progresses by the repeated nucleation of thin platelets often in close proximity to existing platelets, thereby leading to a morphology termed "fault bundles" by other investigators. Individual hcp plates form by the rapid movement of a transformation interface defined by groups of partial dislocations emanating from grain boundaries and non-coherent twin boundaries, and gliding parallel to a given {1 1 1} matrix orientation. The nucleation kinetics are controlled by the thermally activated propagation of partial dislocations originating from boundary networks. It is concluded that short-range diffusion is necessary for the hcp phase to achieve an equilibrium composition, but does not control the rate at which platelets nucleate or propagate.

1. Introduction

Previous studies have shown that the fcc–hcp transformation in metastable Cu–Si and Cu–Ge solid solutions can be activated by isothermal ageing [1–8] or by a lattice displacement mechanism due to applied stress [2, 4, 5, 6, 9, 10]. The mechanisms of the transformation under both sets of conditions have been identified with stacking faults, which are characteristic defects in fcc solid solutions of low stacking fault energy. While the earlier literature stressed the nucleation of the hcp phase at pre-existing matrix stacking faults, more recent work [11–13] points to the importance of the grain boundary as a regenerative source of Shockley partial dislocations which accomplish the change in stacking sequence essential in producing the transformation. This mechanism has been correlated with observations of the fcc–hcp transformation in cobalt [11, 12]. Recent developments in the theory of martensite nucleation [13, 14] are also based on faulting along close packed planes, the fault displacements originating at existing defects such as grain boundaries, incoherent twin boundaries and matrix–inclusion interfaces. For the fcc–hcp transformation the partial dislocations must be spaced two planes apart. Each nucleation event depends on the simultaneous dissociation of a group of dislocations rather than a single dislocation, in order to develop sufficient fault thickness to establish a platelet of the new phase. The thickening of martensite embryos has been described in terms of a "pole" mechanism incorporating existing forest dislocations to produce the necessary increase in dislocation line length without requiring the nucleation of new dislocation loops [14].

Plate thickening under thermally activated or isothermal conditions has been described by models based on profuse faulting [15], ledge growth [8], and a pole-type dislocation mechanism [16–18]. The principal features of several proposals are considered below:

1. Hren and Thomas [15] suggested that the nucleation of the gamma prime phase in Al–Ag alloys occurs from a single matrix stacking fault bounded by Shockley partial dislocations, while thickening occurs by the spontaneous nucleation of other faults adjacent to existing ones. The spontaneous nucleation process was considered to be triggered by lattice strains set up in the matrix as the c/a ratio of the gamma prime changes from 1.633 to 1.59 due to the segregation of silver to the faults. In Cu–Ge alloys, the c/a ratio of the hcp phase is relatively insensitive to germanium content, so this mechanism is questionable as a basis for explaining the thickening process. Aaronson [19] proposed a ledge mechanism which is basically the same as that of Hren and Thomas to account for the transformation in Al–Ag alloys; recent TEM results [17, 18] confirm that plate thickening occurs by ledge migration involving the passage of Shockley partial dislocations.

2. Dahlgren *et al.* [5] postulated that nucleation of the kappa phase in a Cu–4.6 wt % Si alloy occurs from groups of stacking faults formed by the stresses generated during quenching. No model for thickening was proposed.

3. Kasen [4] rejected a glissile partial dislocation mechanism for nucleating the fcc–hcp transformation in the Cu–Si system. He postulated that a high density of Frank sessile loops absorb vacancies during quenching. The loops climb rapidly and convert the

*Present address: Armco Inc., Middleton, Ohio, USA

0022–2461/87 $03.00 + .12

f c c stacking sequence to that of h c p. No such arrays of Frank loops have been observed by TEM in other investigations of Cu–Si alloys [7, 20, 21].

4. Kotval [6] observed bands of h c p structure in surface replicas of Cu–Ge alloys. The bands are formed from identical $a/6\ \langle 1\,1\,\bar{2}\rangle$ shears over several hundred planes of the f c c matrix; similar bands were observed in Co–Ni alloys [22, 23]. Kotval demonstrated that all three shear processes operate on a given $\{1\,1\,1\}$ set of planes and postulated that the bands propagate by means of a "pole mechanism" [24–27] in which a Shockley partial dislocation rotates about a $2a/3\ \langle 1\,1\,1\rangle$ pole dislocation in the f c c structure. The actual nucleation process was not described, nor was any direct evidence of a pole dislocation obtained in thin-foil studies. Furthermore, this mechanism cannot explain the C-curve behaviour exhibited by these alloys. The pole mechanism is thermally activated and should occur quite rapidly at elevated temperatures, but in the upper portion of the C-curve precipitation occurs more slowly with increasing temperature.

5. Kinsman *et al.* [8] reported that the thickening kinetics of kappa plates in Cu–Si alloys cannot be described in terms of the long-range diffusion of silicon to the broad, coherent faces. They also argued that the observed kinetics cannot be described solely by a Shockley partial dislocation ledge mechanism and that the pole model is unlikely on the basis of energy considerations. It was proposed that the kappa plates form from bundles of stacking faults developed by cooling stresses; the faults become enriched with silicon due to short-range diffusion, and limited subsequent thickening may involve the Shockley partial ledge mechanism. TEM and X-ray studies [5, 7] employing slightly lower silicon contents have not revealed the high density of faults needed for dense kappa nucleation following slow cooling from the solution temperature.

It can be argued that a completely coherent equilibrium h c p precipitate should from during ageing by the diffusion of solute to pre-existing faults in a manner described by Suzuki [28]. As diffusion occurs the faults should expand until an equilibrium concentration of solute is reached. However, microscopy studies [2–4, 8] show that platelets having optically resolvable dimensions form spontaneously during the early stages of ageing, suggesting that a mechanism for thickening must occur simultaneously with the edge growth of the plates. The spontaneous generation of faults on every second matrix plane to preserve the h c p stacking sequence was suggested [15] but such an occurrence does not appear plausible unless it occurs in conjunction with a pole mechanism. A mechanism based on lattice strains is also unlikely due to the minimal strain associated with a single fault. Consequently, the concept of nucleation from a single matrix stacking fault is not a viable basis for explaining the observed morphology and kinetics, since questionable thickening mechanisms are required.

The developmental of a reaction model for the thermally induced f c c–h c p transformation in Cu–Ge and Cu–Si alloys must also recognize that the same transformation can be induced by stress in some alloy compositions. Furthermore, the relative contributions of nucleation and growth to the overall transformation kinetics need to be defined. The present paper clarifies some of the controversies concerning the nucleation and growth of h c p plates by employing hot-stage microscopy and TEM techniques to study the transformation in Cu–Ge alloys.

2. Experimental procedure

Cu–Ge alloys containing 10.5 to 12.2 wt % Ge were vacuum-melted and cast into graphite moulds, following which they were homogenized for 30 h at 750° C in an inert atmosphere. The alloys were then cold-rolled, with intermediate anneals, to thicknesses ranging from 1 to 2.5 mm.

Mechanical grinding and polishing of the metastable alloys can induce a phase transformation in the surface layer; consequently, mechanical surface preparation for metallographic studies was limited to cold-worked specimens. Chemical polishing employing a solution of $K_2Cr_2O_7$, NaCl, H_2SO_4 and H_2O proved to be an excellent final preparation stage for solution-treated and aged alloys.

Selective attack by the polish caused grain boundaries, twin boundaries and the zeta phase to stand in relief against the alpha matrix, resulting in brilliant anisotropic effects under polarized light.

The kinetics of zeta plate formation in a Cu–11.8 wt % Ge alloy were studied in a series of thermal cycling experiments involving hot-stage polarized light microscopy [9] at seven temperatures over the range 525 to 350° C. Grains exhibiting good contrast between the zeta phase and the alpha matrix were selected for observation.

The thermal cycling carried out in vacuum or inert gas consisted of a 15 min hold at the solution temperature, followed by quenching to an isothermal ageing temperature between 525 and 350° C. Isothermal ageing was continued until the h c p phase was first detected visually by the appearance of birefringence under polarized light. After holding for an additional ageing period of 10 min the area was photographed and then the specimen was reheated to the original solution temperature. Similar experiments were performed using solution temperatures of 600 and 700° C, and the same range of ageing temperature.

The thin foil specimens for transmission electron microscopy were prepared from heat-treated strips that were thinned electrolytically using the window technique [29]. A solution of 2 parts methyl alcohol and 1 part HNO_3 was used at -40 to -70° C, with no agitation and at a voltage of 8 to 10 V d.c.

The thin foils were examined in a JEM-7 electron microscope operating at 100 kV. A liquid nitrogen cold-finger attachment minimized specimen contamination during observation. A Kikuchi map of reciprocal space was prepared to facilitate an accurate determination of foil orientations and to provide the required consistency between various orientations and operating reflections. The [1 0 0]–[1 0 1]–[1 1 1]–[1 1 0]

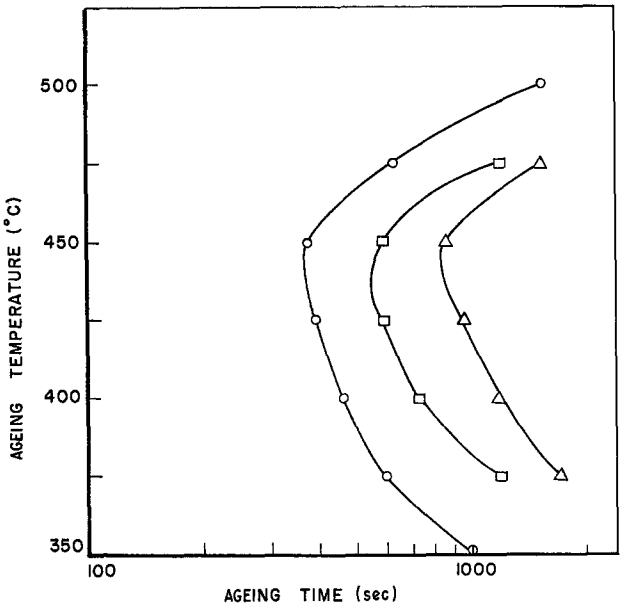

Figure 1 Isothermal transformation curves for a Cu–11.8 wt % Ge alloy solution-treated at (△) 800, (□) 700 and (○) 600° C.

region was chosen for convenience, and the map was prepared using reflections through the {5 1 1} Kikuchi pairs.

3. Experimental results

3.1. Hot-stage microscopy transformation studies

Solution-treated Cu–Ge alloys containing 10.5 to 12.2 wt % Ge exhibited equiaxed recrystallized grains, many of which contained annealing twins. The hcp zeta phase was not detectable under polarized light in these solution-treated specimens. The optical observations were supported by X-ray diffractometer studies on strip specimens and Debye–Scherrer studies on wire specimens, both of which revealed only the presence of the fcc alpha phase.

Ageing 11.8 wt % Ge specimens between 300 and 500° C and the 12.2 wt % Ge specimens between 400 and 650° C produced the platelike hcp zeta phase, identical to that observed by Kotval [3, 6] in Cu–12.5 wt % Ge alloys. The presence of the zeta phase was verified by X-ray diffraction.

The results of the thermal cycling studies are presented graphically in Fig. 1 which indicates C-curve kinetic behaviour for the transformation from supersaturated alpha to the zeta phase. At a given ageing temperature, the time for zeta phase formation increased as the solution temperature increased. A series of transformation experiments conducted on Cu–Si alloys revealed similar C-curve behaviour for kappa phase precipitation. Such C-curve behaviour has not been reported in previous studies [3, 6, 8], probably because the ageing temperatures were either above or below the nose of the C-curve.

The following microstructural features of zeta phase formation were noted during the hot-stage studies:

1. For a given ageing time, the amount of transformation varied from grain to grain.
2. The zeta plates had already attained their final length when first observed at 200×, i.e. the length of the plates did not change with ageing time.
3. When ageing was carried out above the nose of the C-curve the transformation product consisted of very fine platelets. As the ageing temperature was decreased, the numbers of zeta plates increased, with an attendant loss of resolution of the individual plates or groups of plates.
4. It was not possible to monitor the thickening of the individual platelets at 200× in the hot stage. However, the optically thick plates of zeta were actually composed of a number of fine laths, as shown in Figs 2a and b, suggesting that microscopic thickening occurs by the formation of new plates adjacent to those formed initially, rather than by the continued growth of older platelets.

At no time was a morphology other than long, straight striations observed in any of the alloys; for example, no globular precipate was ever observed at grain boundaries. In addition, no denuded or precipitate-free zones were ever observed in the quenched and aged alloys, although such observations are common in other alloy systems [30, 31].

Some zeta platelets are terminated by grain boundaries as at A in Fig. 3a, or by a grain boundary at one end and by a twin boundary or another colony of zeta

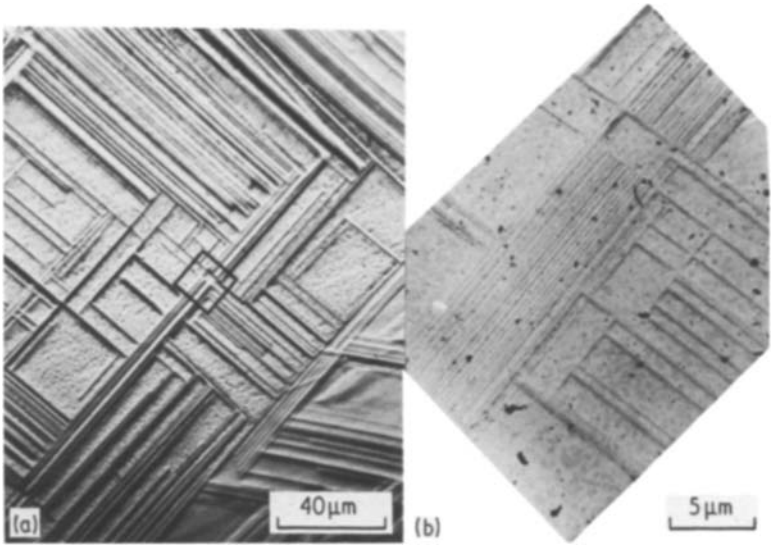

Figure 2 Cu–11.8 wt % Ge alloy solution-treated at 800° C and aged at 450° C for 1 h. (a) Polarized light optical micrograph showing "optically thick" zeta plates. (b) Replica TEM micrograph of area in box in (a) showing that an "optically thick" plate is actually composed of many finer platelets.

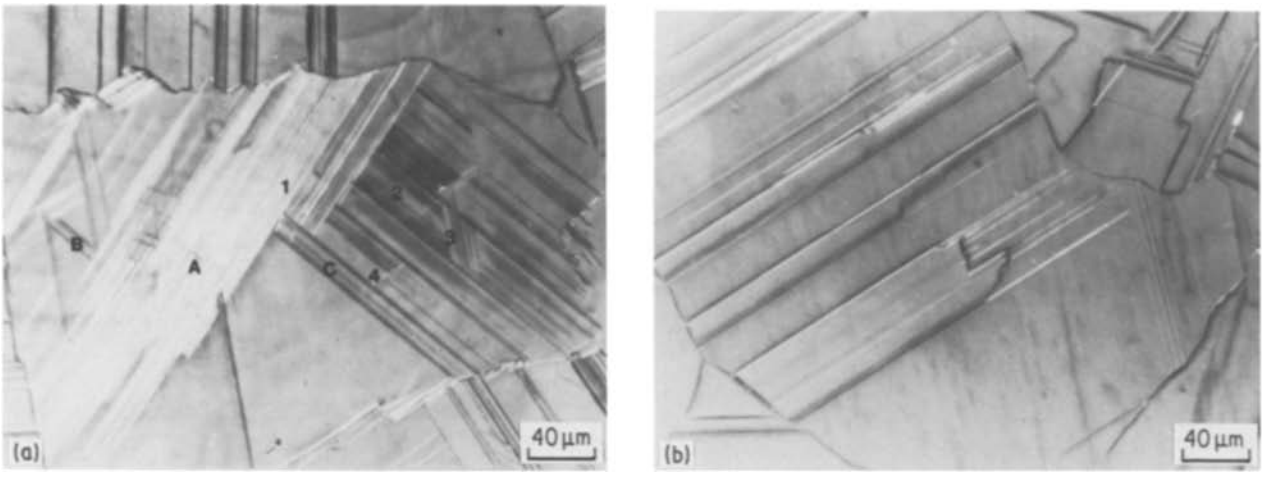

Figure 3 Cu–11.8 wt % Ge solution-treated at 800° C and aged at 450° C for 1h. (a) Polarized light optical micrograph showing four variants (1 to 4) of zeta phase within a grain. (b) Polarized light optical micrograph showing zeta phase which emerged from a non-coherent boundary of an annealing twin.

plates at the other end, as at B in Fig. 3a. Zeta platelets were also observed to emerge from the incoherent boundaries of twins, as shown in Fig. 3b.

3.2. Effect of quenching on subsequent ageing

In order to determine whether the alpha to zeta transformation exhibited a quench-rate sensitivity, Cu–12.2 wt % Ge sheets were solution-treated at 800° C for 2 h, cooled in various media, and subsequently aged at 450° C for 30 min. The cooling media were iced brine at 0° C, still oil, air, and vacuum. None of the specimens exhibited zeta phase in the microstructures at room temperature after direct cooling from 800° C; also, there was no evidence of slip indicative of plastic deformation during the quench, and strain-induced zeta phase was never observed.

The microstructures following ageing are shown in Figs 4a to d; brine- and oil-quenched specimens exhibit much more anisotropy than either the air- or vacuum-quenched specimens, suggesting that the alpha to zeta transformation is accelerated by high rats of quenching.

The appearance of the zeta platelets varied with the cooling rate from the solution temperature, as can be seen by comparing Figs 4a and 4d. After brine-quenching and ageing the entire surface exhibited a high density of fine striations under polarized light, as shown in Fig. 4a; many subregions of the four possible variants have also formed within a grain. In the vacuum-cooled and aged specimen shown in Fig. 4d, much less optical anisotropy is evident and the striations appear coarser than those in the quenched specimen; also fewer subregions have formed within any given grain.

3.3. Electron microscopy studies

3.3.1. Early stages of ageing

Electron microscopy studies revealed intrinsic stacking faults to be the principle lattice defects in slowly cooled Cu–Ge alloys containing 10.8 to 12.2 wt % Ge. Brine-quenching from the solution temperature produced a variety of defects, including intrinsic faults, "ragged" Shockley partials and black spot defects; the latter were attributed to quenching strains and vacancy migration effects. The zeta phase was not detected in the solution-treated alloys by electron microscopy and selected-area diffraction techniques. Low-temperature ageing studies revealed the formation of stacking-fault tetrahedra due to vacancy clustering prior to the detection of zeta phase formation. These observations and phenomena have been discussed in adequate detail elsewhere [32, 33].

At all ageing temperatures, the random faulting

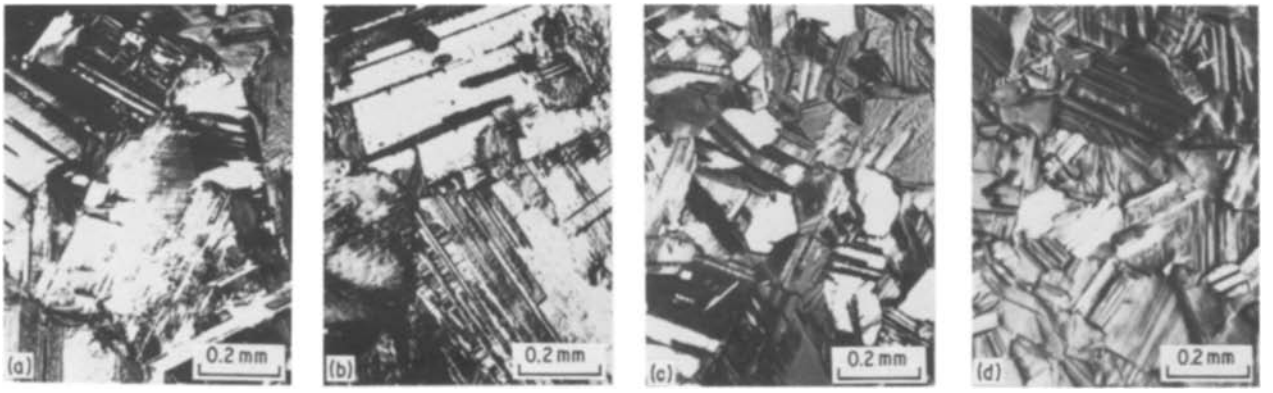

Figure 4 Cu–12.2 wt % Ge solution-treated at 800° C, quenched in various media and aged at 450° C for 30 min. Polarized light optical micrographs of (a) iced brine quenched, (b) oil quenched, (c) air cooled, (d) vacuum cooled specimens.

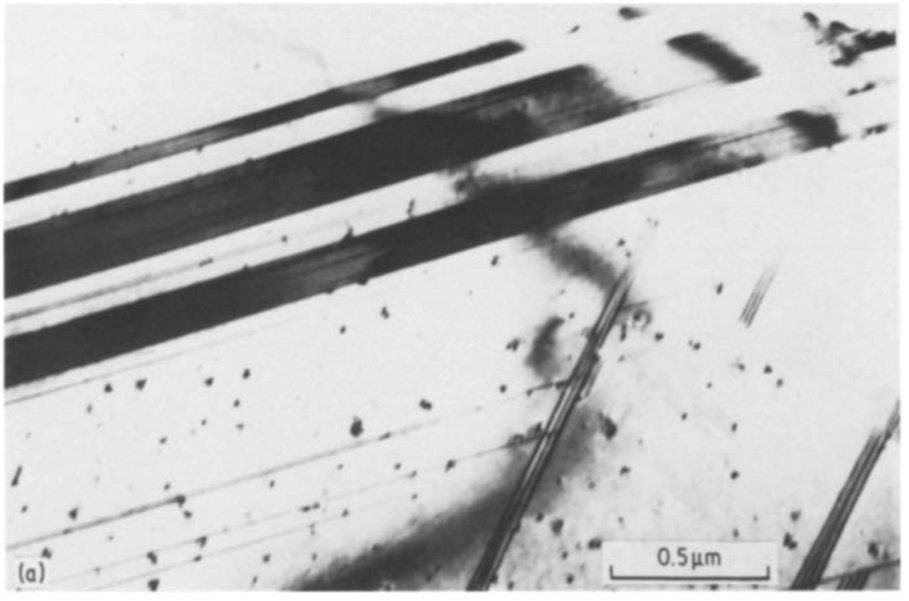

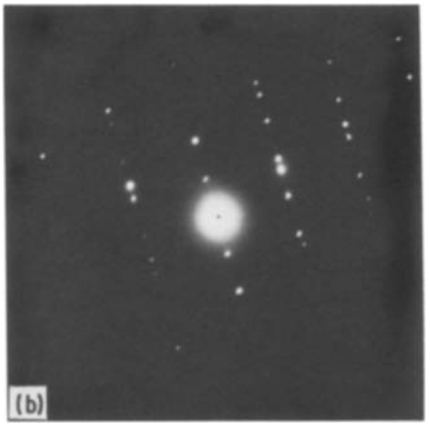

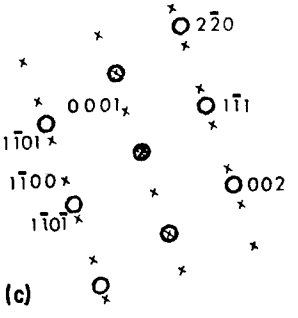

Figure 5 Cu–12.2 wt % Ge solution-treated at 800° C, iced brine quenched and aged at 450° C for 96 h. (a) Bright-field TEM micrograph of the zeta (hcp) phase showing deviations in the matrix Bragg contours as the platelets cross the hcp phase. (b) SAED pattern of (a). (c) Solution of (b); (○) [1 1 0] fcc, (×) [$\bar{1}\,\bar{1}$ 2 0] hcp.

present in solution-treated and slow-cooled or quenched specimens was replaced by non-random faulting in the form of "bundles of faults" which become quite massive and better defined as ageing proceeded. After long ageing times near 450° C, the zeta phase could be detected by observing deviations in matrix Bragg extinction contours as they crossed the hcp phase; this behaviour has been described by Delaey [34]. The zeta phase was generally faulted to some extent even after long ageing times, as evident in Fig. 5a after ageing for 96 h at 450° C. The diffraction pattern and the indexing shown in Figs 5b and c, respectively, verify that both the alpha and zeta phases are present.

After short ageing times, it was not possible to distinguish between the zeta phase regions and areas of very high stacking-fault density in the electron micrographs. Furthermore the selected-area electron diffraction (SAED) patterns were complicated by the satellite spots produced by the stacking faults in heavily faulted areas [35, 36].

When SAED was performed on "bundles of faults" formed on planes normal to a ⟨1 1 0⟩ foil zone, the following sequence of changes occurred with increasing ageing time, as shown in Figs 6a to d:

1. Continuous streaking occurred from one matrix spot to another along ⟨1 $\bar{1}$ 1⟩ directions. The streaks often exhibited fine maxima which "moved" as the foil orientation was changed slightly. Such maxima did not occur preferentially where hcp diffraction spots were expected.

2. Shortening of the streaks occurred and intensity maxima developed gradually at positions corresponding to the expected reflections from hcp zeta phase. Kotval and Honeycombe [3] used the appearance of the {1 0 $\bar{1}$ 0} zeta reflection as the criterion for the presence of zeta phase; this reflection is isolated from other diffraction spots and cannot be produced by the broadening of matrix reflections [37]. However, this criterion is limited to platelets having sufficient thickness to produce detectable {1 0 $\bar{1}$ 0} maxima during electron diffraction.

3. Well-defined zeta reflections were observed, including {1 0 $\bar{1}$ 0} and {0 0 0 1} "forbidden" reflections caused by double diffraction; some streaking occurred due to the small thickness of the zeta platelets.

When SAED was performed on "bundles of faults" on planes inclined to a ⟨1 1 0⟩ foil zone, the presence of zeta phase was confirmed by the appearance of a ⟨2 2 $\bar{4}$ 3⟩ zeta zone axis pattern superimposed on the ⟨1 1 0⟩ alpha zone axis pattern. Since the {1 $\bar{1}$ 0 0}

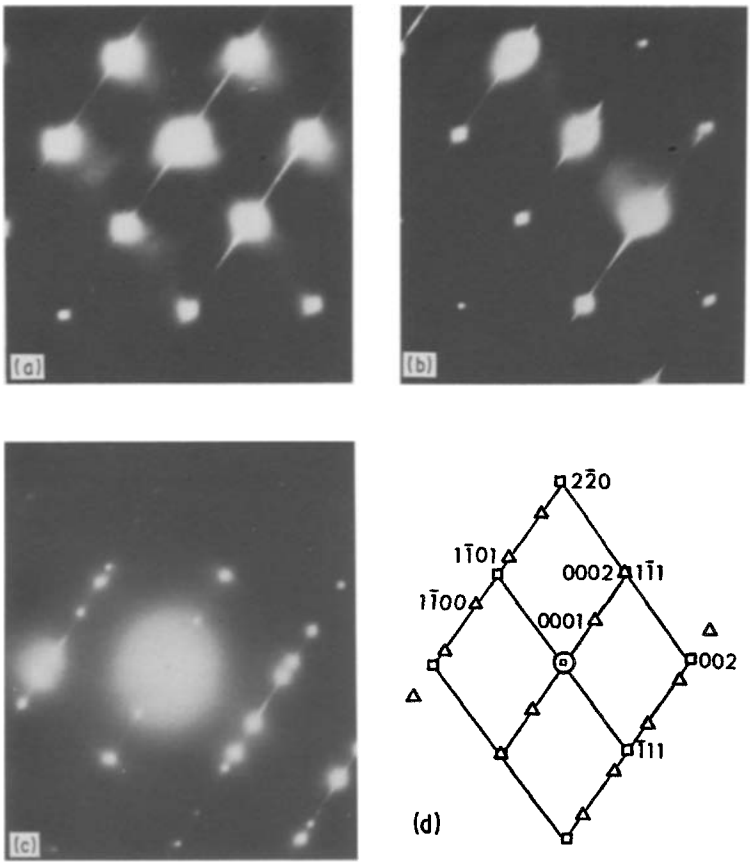

Figure 6 SAED patterns of a foil in [1 1 0] orientation illustrating the changes in pattern with ageing time. (a) Continuous streaking in the [1 $\bar{1}$ 1] direction. (b) Shortening of streaks and development of maxima near [1 1 $\bar{2}$ 0] zeta positions. (c) Superimposed [1 1 0] f c c and [1 1 $\bar{2}$ 0] h c p zones. (d) Solution of (c); (□) [1 1 0] f c c, (△) [1 1 $\bar{2}$ 0] h c p.

reflection belongs to the $\langle 2\,2\,\bar{4}\,3\rangle$ zone axis family, the presence of a $\{1\,0\,\bar{1}\,0\}$ reflection is a valid basis for identifying the formation of the zeta phase.

When non-$\langle 1\,1\,0\rangle$ matrix zone axes were observed, it was necessary to calculate the possible zeta zone axes that were parallel to a given (u v w) matrix zone. If a zeta zone containing low-index diffracting planes were present (e.g. $\{0\,0\,0\,1\}$, $\{1\,0\,\bar{1}\,0\}$, $\{1\,\bar{1}\,0\,0\}$, $\{1\,0\,\bar{1}\,1\}$), a discrete h c p zone axis pattern could be observed. If the predicted zone axis pattern did not contain low index planes, but was near a zone in reciprocal space that did contain low index planes, rel-rods from this latter zone often intercepted the pattern. In many cases it was not possible to determine whether certain diffraction spots in a given pattern were rel-rods from the zeta phase or from "bundles of faults" without tilting the foil to a different orientation.

3.3.2. Zeta phase formation in slow-cooled alloys

The first positive identification of zeta phase occurred after ageing at 450° C for 15 mins, as shown in Figs 7a to c. The zeta phase platelets exhibited thicknesses of only 4.5 to 30 nm, but clearly cause deviations in the matrix Bragg extinction contours as shown in Fig. 7a. It is not clear whether the platelet in Fig. 7a is a single plate containing internal faults, or two platelets separated by a small volume of matrix. The selected-area diffraction pattern, as shown in Fig. 7b, contains a [1 1 $\bar{2}$ 0] h c p zone axis pattern, which exhibits (0 0 0 1) and $\{1\,\bar{1}\,0\,0\}$ diffraction spots, confirming the presence of zeta phase. The nearly continuous streaking occurs because the platelets of zeta are extremely fine. These platelets were bound by the foil edge at one end and terminated on the coherent boundary of an annealing twin on the other, as shown in Fig. 8.

When the ageing time was increased to 30 min, the number of platelets, as well as the maximum thickness (~ 70 nm) increased, as shown in Fig. 9. Continued ageing for 1 h produced very large platelets such as those in Fig. 10a. The edge attack is due to preferential dissolution of the matrix during the thinning process and is interpreted as an indication of compositional variation [7]. The orientation of the laths in Fig. 10a is $\{1\,1\,\bar{2}\,3\}$; the diffraction pattern and its solution are shown in Figs 10b and c, respectively.

When ageing was carried out below the nose of the C-curve at 400° C for 2 h, zeta plates similar to those observed at 450° C were seen. A view of the zeta plates in a [1 0 0] foil is shown in Fig. 11a. The relative continuity of the matrix Bragg extinction contour eliminates the possibility that these are twins, as does the diffraction pattern of Fig. 11b, which is not the [1 1 0]–[2 2 1] combination expected for twinning on (1 1 1) in a [1 0 0] orientation. Note the development of satellite spots around the matrix spots, and the partial streaking.

Similar observations hold true for ageing at 500° C for 2 h, although few zeta plates were observed for this ageing treatment.

3.3.3. Zeta phase formation in brine-quenched alloys

3.3.3.1. Aged at 450° C for 30 min. The results of optical microscopy, as shown in Fig. 4, indicated that zeta phase forms more rapidly and in greater amounts in alloys that are brine-quenched as compared to those which are air-cooled. Fig. 12a illustrates the complexity

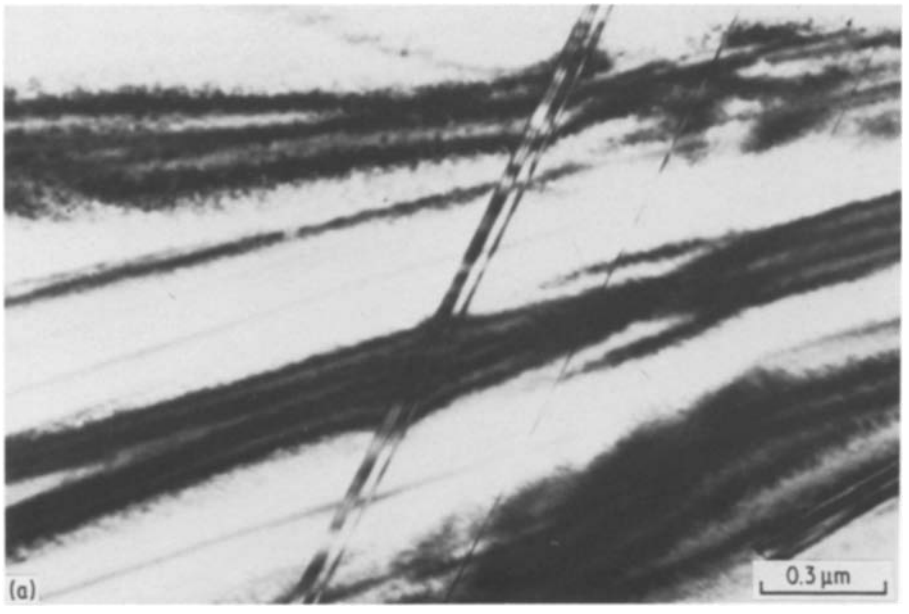

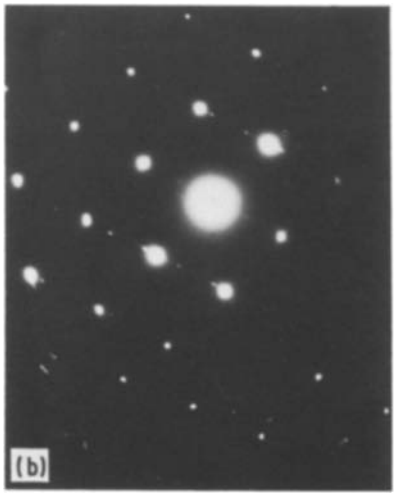

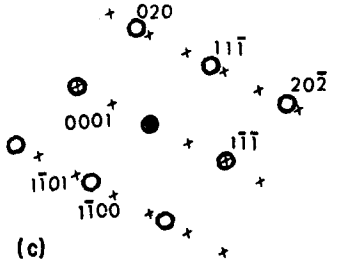

Figure 7 Cu–11.8 wt % Ge solution-treated at 800° C, cooled in vacuum to 450° C and aged for 15 min. (a) Bright-field TEM micrograph of the first observed zeta platelets. (b) SAED pattern of (a); [1 0 1] fcc and [1 1 $\bar{2}$ 0] hcp zones. (c) Solution of (b); (○) [1 0 1] fcc, (×) [1 1 $\bar{2}$ 0] hcp.

of structure produced by ageing a Cu–12.2 wt % Ge alloy for 30 min at 450° C following an iced-brine quench. Fig. 12a shows faulting to different degrees on all four {1 1 1} variants. The faulting is particularly heavy on the (1 $\bar{1}$ 1) planes and the (1 1 $\bar{1}$) planes, corresponding to "bundles of faults" on these planes. The SAED pattern in Fig. 12b contains a [1 0 1] fcc zone, a [1 1 $\bar{2}$ 3] hcp zone and a [1 1 $\bar{2}$ 0] hcp zone, as shown in the solution to this pattern in Fig. 12c. The presence of {1 $\bar{1}$ 0 0} zeta reflections in each of these patterns, as well as the patterns themselves, show that the "fault bundles" are in fact the hcp zeta phase. High resolution dark-field images taken from {1 $\bar{1}$ 0 1} reflections of the two zeta variants are shown in Figs 13a and b. The zeta phase on (1 1 $\bar{1}$) appears to have partially penetrated the zeta phase on (1 $\bar{1}$ 1) on the

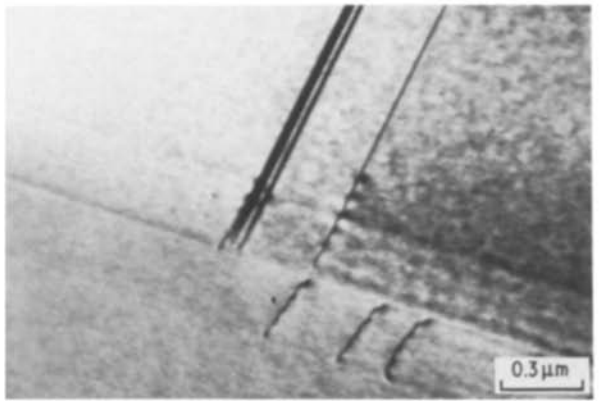

Figure 8 Bright-field TEM micrograph of the zeta platelets in Fig. 7a showing the termination of one end of the platelets at a coherent annealing twin boundary. The other end terminated at the foil edge.

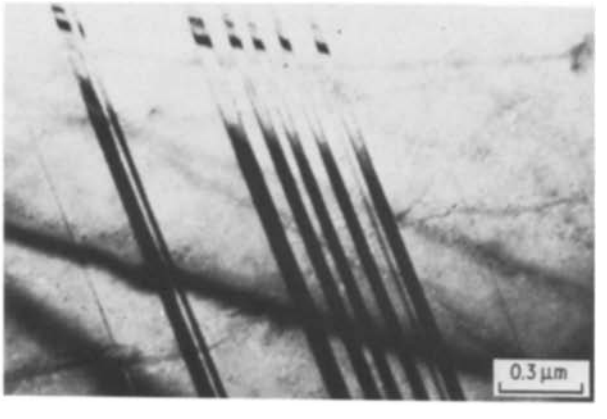

Figure 9 Cu–11.8 wt % Ge solution-treated at 800° C, vacuum cooled to 450° C and aged for 30 min. Bright-field TEM micrograph of a cluster of zeta platelets.

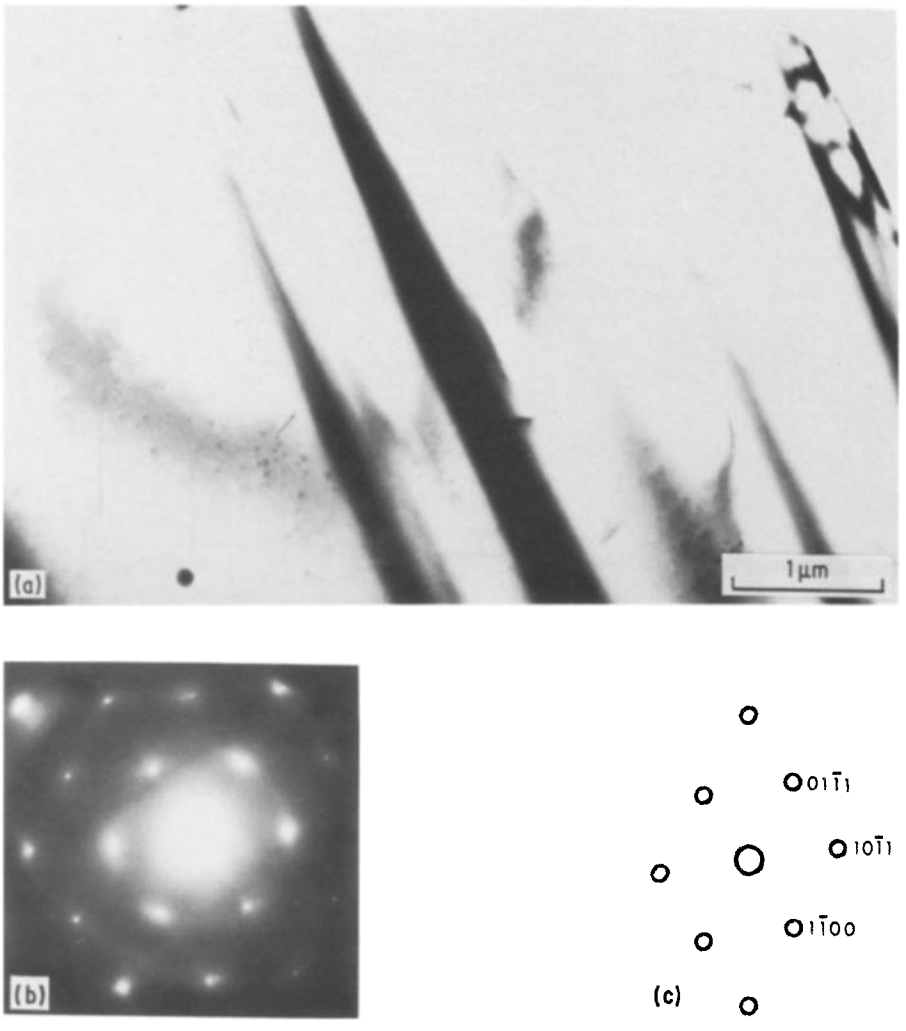

Figure 10 Cu–11.8 wt % Ge solution-treated at 800° C, vacuum cooled at 450° C and aged for 1 h. (a) Bright-field TEM micrograph of zeta platelets. (b) SAED pattern of (a) showing a $[1\,1\,\bar{2}\,3]$ zeta zone. (c) Solution of (b); $[1\,1\,\bar{2}\,3]$ h c p.

left. It is not certain whether the stresses generated caused nucleation of more zeta on $(1\,1\,\bar{1})$ to the right, or whether the nucleating site of the $(1\,1\,\bar{1})$ zeta was below that on $(1\,\bar{1}\,1)$ and other obstructions limited zeta phase growth on the right-hand side.

Tilting the foil so that $\bar{g} = (1\,\bar{3}\,\bar{1})$ is operating, as shown in Fig. 13c, reveals the zeta phase on $(1\,\bar{1}\,1)$. It is not certain whether the dislocation segments evident in Fig. 13c are associated with the transformation itself, or whether they are the result of zeta phase impingement involving different habit orientations. The contrast in the zeta on $(1\,1\,\bar{1})$ indicates that what appears to be a thick plate is actually many thin ones in close proximity, thereby suggesting that the apparent "stacking fault bundles" in the zeta phase are actually due to an interference effect from the interfaces of very closely spaced plates. The irregular shapes of the tips of the zeta plates on $(1\,1\,\bar{1})$ suggest that the platelet edges are defined by incoherent interfaces.

3.3.3.2. Aged at 300° C for 22 h. The zeta phase was detected after 22 h at 300° C, as demonstrated in Figs 14a and b, where "bundles of faults" were verified as zeta phase by the $[1\,1\,\bar{2}\,0]$ h c p pattern of the SAED pattern. When the orientation was not ideal for obtaining a low-index zeta zone axis, the pattern contained matrix spots with satellite spots close by.

Fig. 15a shows a grain boundary containing periodic lines which resemble defects identified by others [38–40] as grain-boundary dislocations. Of particular interest are the faults in the lower grain which intersect the boundary precisely parallel to these periodic lines, clearly suggesting that these faults resulted from the glide of boundary dislocations into the matrix. When the foil was tilted to near the [5 2 1] matrix zone, a $[1\,1\,\bar{2}\,3]$ h c p pattern was revealed, as shown in Figs 15b and c, clearly indicating that the "faults" are actually a series of thin zeta plates. The corresponding bright-field image is shown in Fig. 15d.

4. Discussion

4.1. Microstructural processes

The shapes of the isothermal transformation curves shown in Fig. 1 for the initiation of decomposition in Cu–Ge alloys suggest classical nucleation and growth behaviour. An analysis of the present work, in conjunction with the work of others [8], clearly demonstrates that the transformation kinetics are not classical nucleation and growth processes. The following points are important:

1. Classical nucleation and growth behaviour is expected to be controlled by diffusion at lower temperatures. If this is so, then a plot of $\ln t$, where t is the time at which platelets were first observed in the microstructure, plotted against $1/T$, where T is the absolute temperature, should be linear. A linear

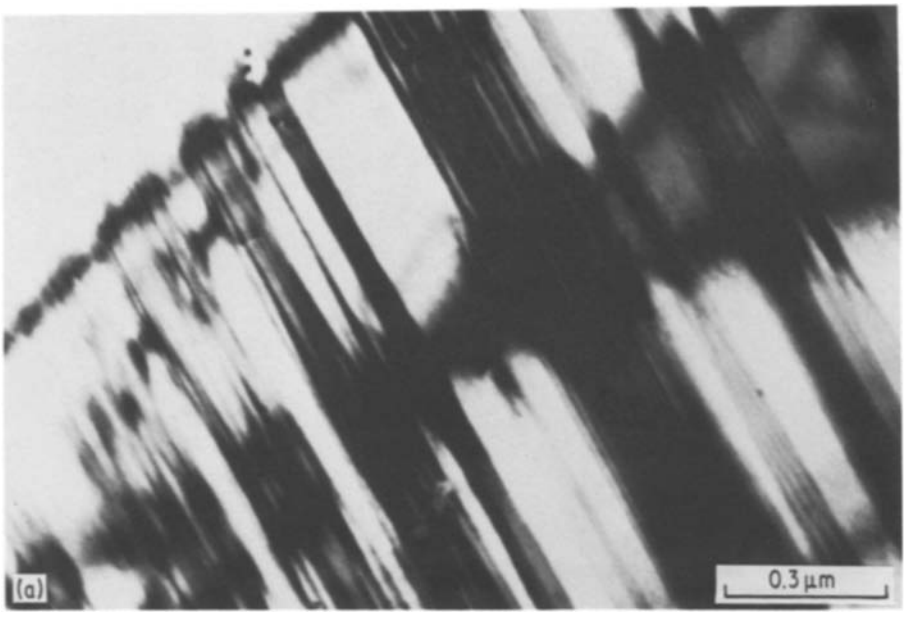

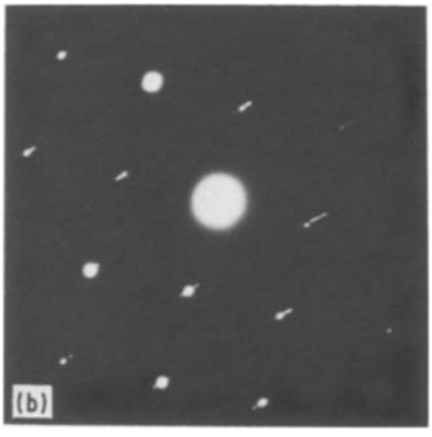

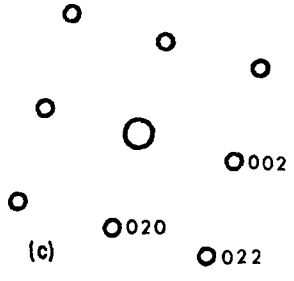

Figure 11 Cu–11.8 wt % Ge solution-treated at 800° C, vacuum cooled to 400° C and aged for 12 h. (a) Bright-field TEM micrograph of fine zeta platelets in a [1 0 0] foil. (b) SAED pattern of (a). Note the satellite spots around the matrix spots. (c) Solution of (b); [1 0 0] fcc.

relationship does not result from the data of Fig. 1, suggesting that the kinetics are not dependent on diffusion alone.

2. When the zeta-phase plates were first resolved at optical magnifications in the hot stage, they had already achieved their full length.

3. In a study of plate thickening in the similar Cu–Si system Kinsman *et al.* [8] showed the thickness increase occurred in discrete jumps rather than as a continuous process, a result not expected for simple diffusion-controlled growth.

4. Both TEM and optical observations indicate that zeta plates always terminate at microstructural barriers, generally a coherent twin boundary, a grain boundary, or interception with a colony of zeta plates forming on another {1 1 1} habit plane (Fig. 8).

5. TEM observations indicate the initial zeta platelets to be extremely thin, i.e. approximately 5 to 30 nm. Also, as shown in Fig. 7a, the deviation of the Bragg contours within the thickest plate suggests that it actually comprises two or three thinner plates in close proximity.

6. Continued ageing produces a progressively increasing density of plates; deviations in Bragg contours again suggest that the thickest plates are composed of several finer plates in close proximity.

7. The zeta phase was observed to form at the same sites in a reversible manner during thermal cycling, implying that the same nuclei were being activated.

The above observations point to the importance of nucleation as the rate-controlling factor in the formation of the hcp phase from supersaturated alpha phase in both the Cu–Ge and Cu–Si systems. Such behaviour is not unique to these two systems. The isothermal transformation of fcc austenite to bct martensite in an Fe–23 Ni–4 Mn alloy has been observed to exhibit C-curve behaviour [41, 42]. The growth rate in this alloy and in similar alloys [42] is quite rapid and independent of the transformation temperature; that is, the growth rate is not diffusion-controlled and is in fact martensitic. Olson and Cohen [13, 14] explain the kinetics in terms of triggering the growth of embryos formed by a faulting process derived from a group of existing dislocations. In this sense, the transformation process is considered an operational problem rather than a problem of forming a stable nucleus and causing it to grow.

4.2. A model for the fcc–hcp transformation by movement of a "transformation interface"

Due to the similarity of stacking faults and an hcp phase, it is natural to consider the fcc–hcp

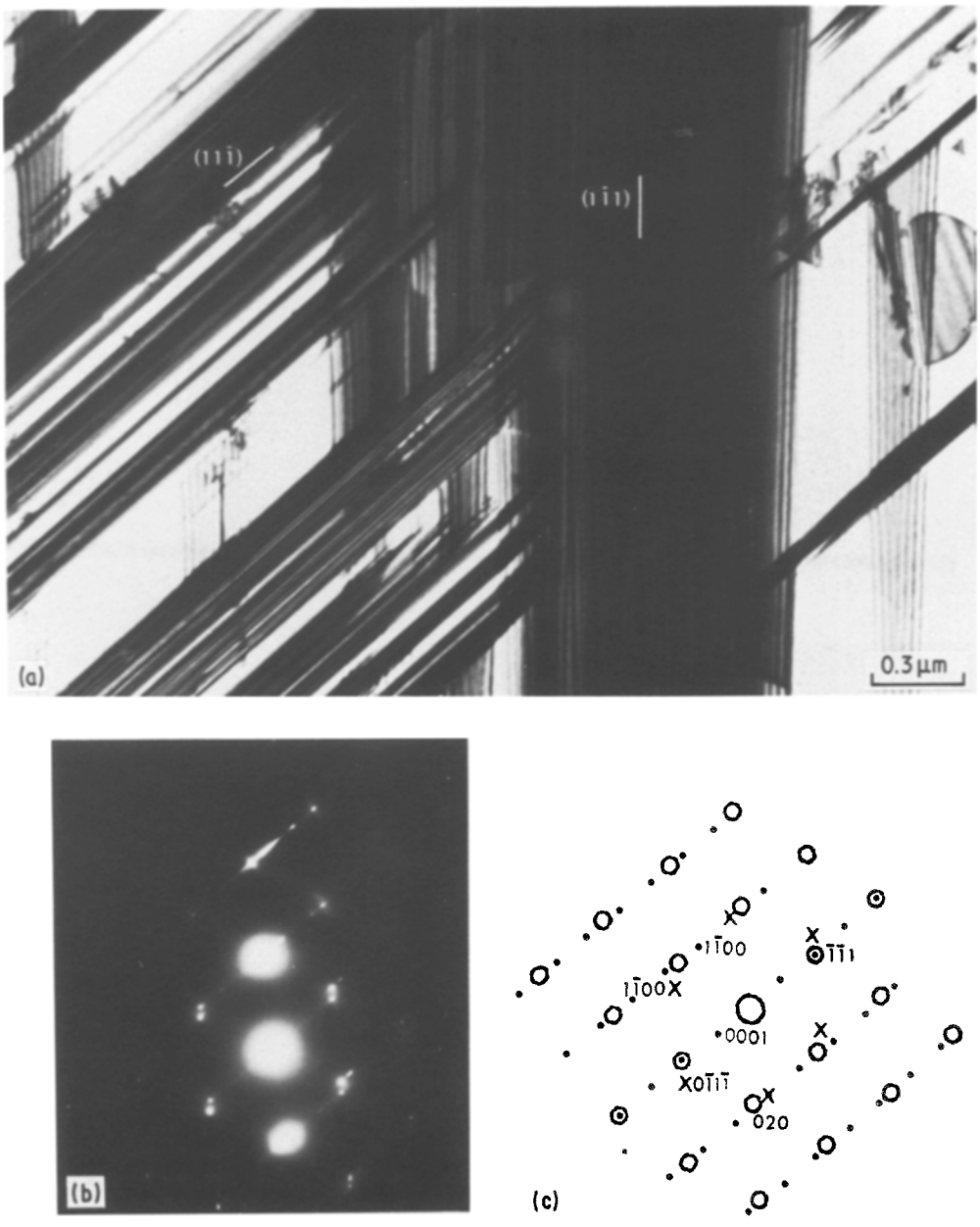

Figure 12 Cu–12.2 wt % Ge solution-treated at 800° C, iced brine quenched, and aged at 450° C for 30 min. (a) Bright-field TEM micrograph of two variants of zeta phase, one on (1 1 $\bar{1}$) and one on (1 $\bar{1}$ 1). Faulting on the other {1 1 1} planes is evident. (b) SAED pattern of (a) showing [1 0 1] f c c zone, [1 1 $\bar{2}$ 0] h c p zone for zeta on (1 1 $\bar{1}$) and [1 $\bar{2}$ 1 3] h c p zone for zeta on (1 $\bar{1}$ 1). (c) Solution of (b); (○) [1 0 1] f c c, (●) [1 1 $\bar{2}$ 0] h c p, (×) [1 1 $\bar{2}$ 3] h c p.

transformation in terms of the movement of glissile Shockley partial dislocations on alternate {1 1 1} planes of the f c c lattice. Viewing the transformation in this manner results in the dilemma that no obvious method for thickening of the h c p phase appears to exist. The zeta and kappa phases in Cu–Ge and Cu–Si, respectively, are both separated from the f c c matrix by coherent boundaries; consequently, insufficient strain fields exist to cause the nucleation of additional layers in the early stages of formation. Even after long periods of ageing, interfacial dislocations are not observed at the zeta–alpha interfaces in Cu–12.5 wt % Ge [6] or at the kappa–alpha interfaces in Cu–5.09 wt % Si [8], indicating that coherency is maintained.

Kinsman *et al.* [8] postulated that "bundles of faults" produced by quenching strains in a quenched Cu–5.09 wt % Si alloy acted as the nuclei for the transformation. In the present study, slow cooling to room temperature produced no "bundles of faults" in Cu–11.8 wt % Ge alloys, nor were "bundles of faults" observed in aged samples. The first manifestation of the zeta phase, as illustrated in Figs 7 and 8, was the appearance of very fine (~3 nm) relatively perfect h c p platelets. Thickening detected at the optical microscopy level was confirmed by TEM to occur by the formation of additional thin h c p platelets adjacent to those previously formed. If a large number of thin platelets form close to one another, the resultant configuration leads to the appearance of a "bundle of faults". It is believed that the "bundles of faults" observed by Kinsman *et al.* [8] and Kotval [6] are actually clusters of thin platelets in close proximity. An example of such plate clusters and their similarity to "bundles of faults" is illustrated in Fig. 12 for a quenched and aged Cu–12.2 wt % Ge alloy.

The formation of a thin discrete h c p platelet can occur by the movement of a glissile "transformation interface" through the f c c matrix. The interface must

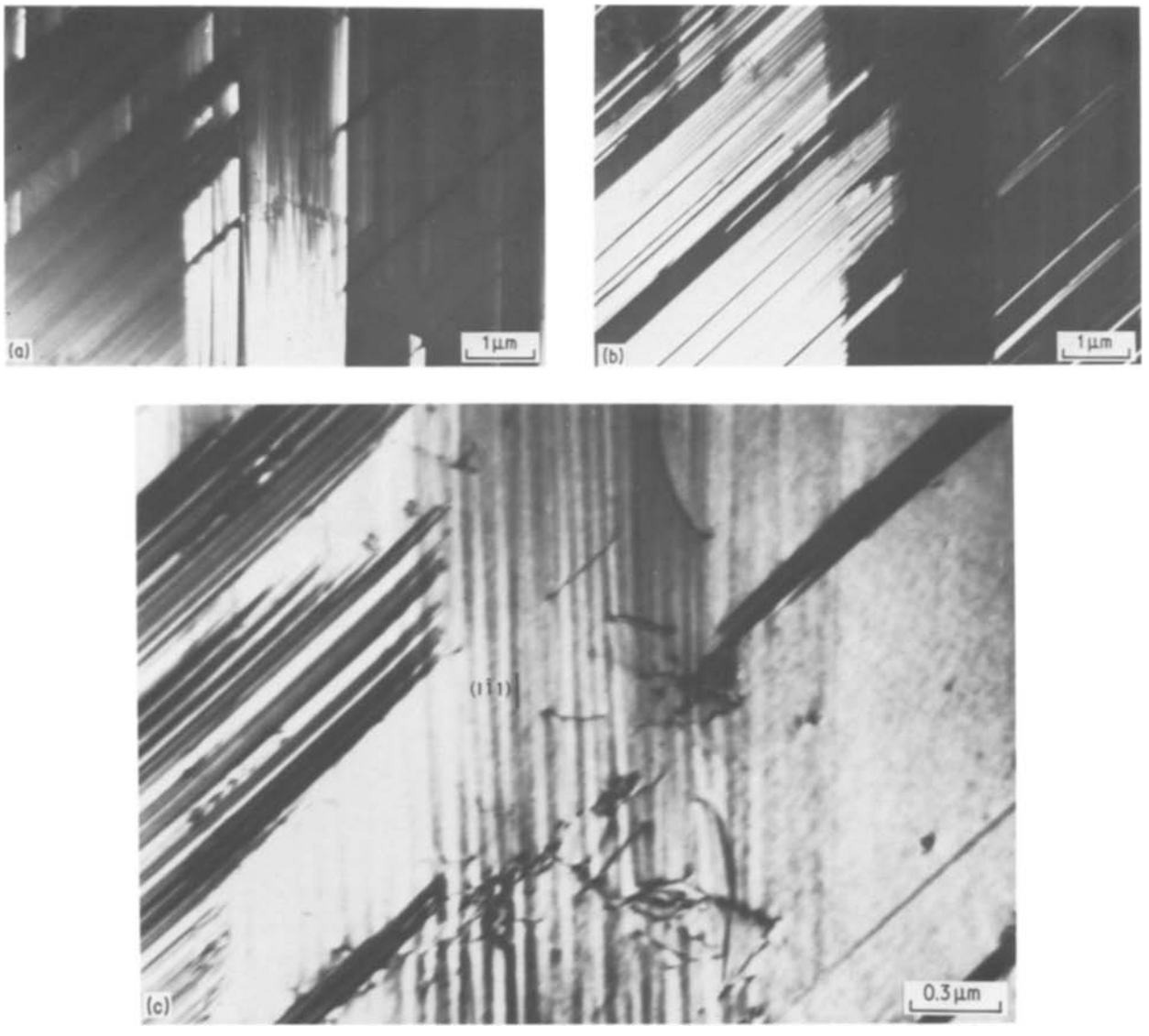

Figure 13 Cu–12.2 wt % Ge solution-treated at 800° C, iced brine quenched, and aged at 450° C for 30 min. (a) Dark-field TEM micrograph imaged from (0 1 $\bar{1}$ 1) h c p reflection in [1 $\bar{2}$ 1 3] h c p zone, showing zeta on (1 $\bar{1}$ 1). (b) Dark-field TEM micrograph imaged from (1 $\bar{1}$ 0 1) h c p reflection in [1 1 $\bar{2}$ 0] h c p zone, showing zeta on (1 1 $\bar{1}$). (c) Bright-field electron micrograph of the intersection of the two variants of zeta phase shown in (a). The fringes for the zeta on (1 $\bar{1}$ 1) are invisible for $\vec{g} = \bar{1}\,3\,\bar{1}$, but some residual contrast from the thin platelets remains.

be composed of a group of dislocations which can glide rapidly and simultaneously through the f c c matrix to convert the f c c stacking sequence to that of h c p. In order to produce the proper stacking sequence and to maintain a net shear of zero, which is required to ensure the coherency of the interface on the {1 1 1} planes, the Burgers vectors are required to have specific relationships, as proposed by Horsewell *et al.* [11, 12].

The passage of the transformation interface produces a thin h c p platelet of finite thickness. Additional platelets form with the passage of additional transformation interfaces, producing the morphologies illustrated in Figs 2b, 7 and 12. The model also negates the necessity for layer-by-layer thickening of the h c p platelets, since each nucleated platelet has a definite thickness determined by the number of partials in the group participating in a particular glide event.

Each transformation interface moves through the lattice until it encounters a barrier to further propagation. Such barriers can be platelets on other orientations, grain boundaries, or twin boundaries, in keeping with the morphology observations.

This transformation interface mechanism would produce the h c p phase with an ideal c/a ratio. Since the c/a ratio of both the zeta and kappa phases is nearly ideal [4, 6, 8], only a small amount of short-range solute diffusion is required to establish equilibrium compositions.

4.3. Nucleation sites for the f c c–h c p transformation

Single intrinsic stacking faults were the only major imperfection observed within the f c c matrix grains of a Cu–11.8 wt % Ge alloy in the solution-treated and slow-cooled condition. These individual faults are unlikely nucleating sites on the basis of the high fault densities required to accommodate the transformation and the inability of individual faults to account for the observed morphological characteristics of the h c p phase. Grain boundaries and non-coherent twin boundaries, both of which are known to contain

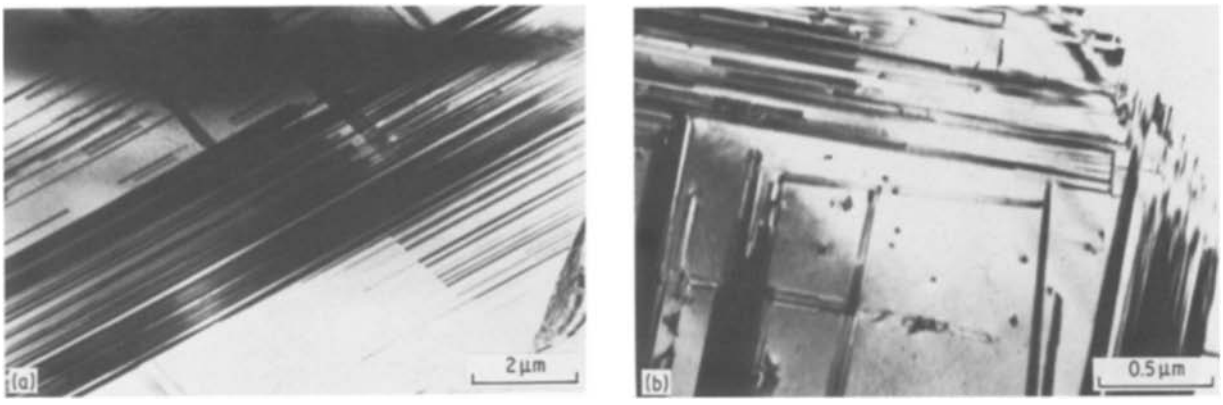

Figure 14 Cu–12.2 wt % Ge solution-treated at 800° C, quenched in iced brine, and aged at 300° C for 22 h. (a) Bright-field TEM micrograph of a cluster of zeta platelets. [1 1 0] zone. (b) Bright-field TEM micrograph of clusters of zeta platelets in a [1 0 0] foil.

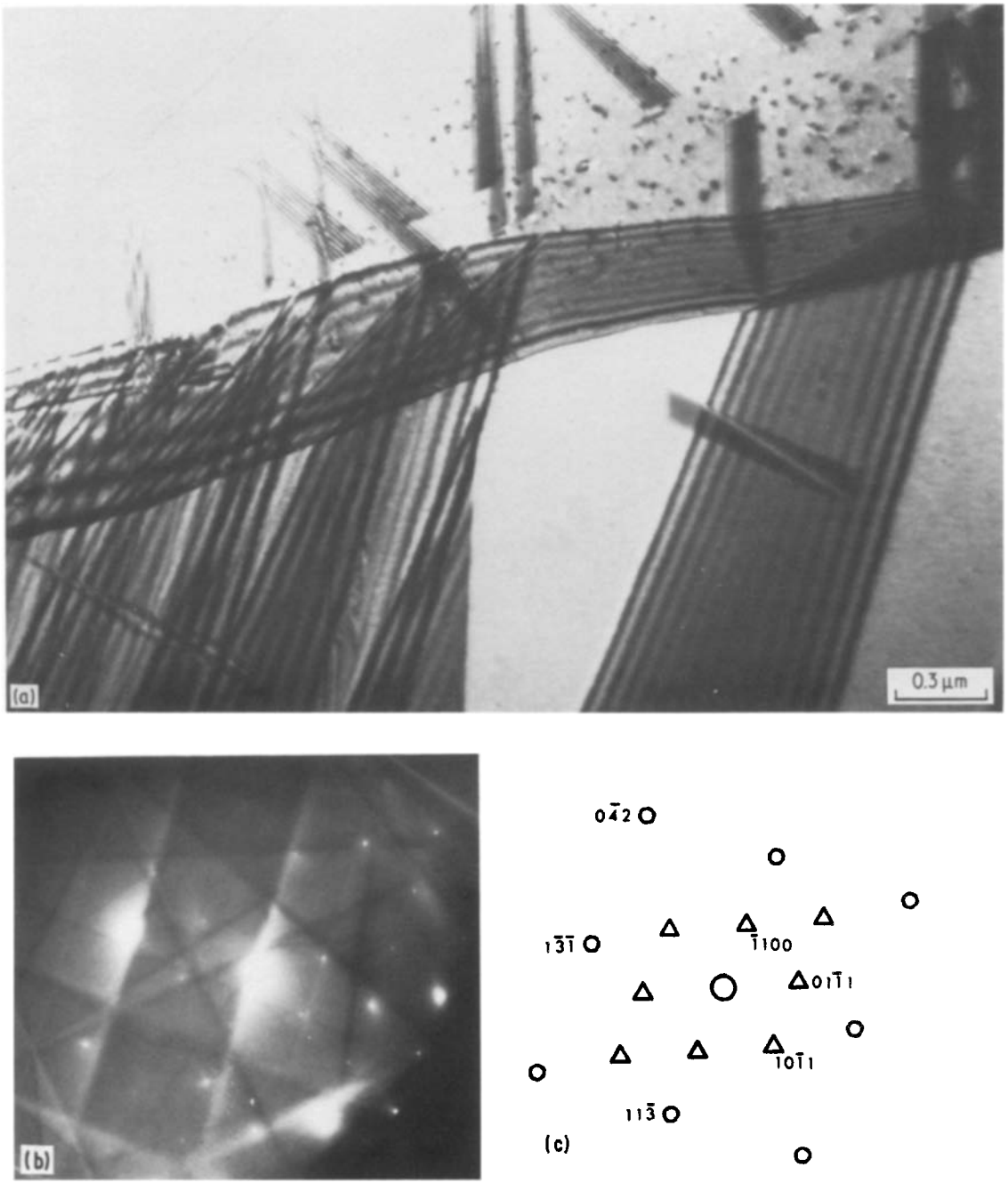

Figure 15 Cu–12.2 wt % Ge alloy solution-treated at 800° C, iced brine quenched, and aged at 300° C for 22 h. (a) Bright-field TEM micrograph showing a grain boundary containing periodic lines. The intersection of the fringes with the boundary is parallel to the periodic lines. [1 1 0] zone $\bar{g} = 1\bar{1}\bar{1}$. (b) SAED pattern of (a) after tilting to [5 2 1]. The [1 1 $\bar{2}$ 3] h c p zone shows that the fringes in (a) are zeta platelets. (c) Solution of (b); (○) [5 1 2] f c c, (△) [1 1 $\bar{2}$ 3] h c p.

dislocation networks [43], remain as the most probable nucleating sites.

Earlier experiments [4] on Cu–Si alloys revealed that no transformation occurred in a Cu–4.65 wt % Si alloy after slow cooling to room temperature, but some transformation did occur under identical conditions in a Cu–5 wt % Si alloy. Increasing the solute content lowers the stacking fault energy (SFE) of Cu–Si and Cu–Ge alloys [20, 21, 44, 45]. For example, the SFE for a stable Cu–10.5 wt % Ge alloy is about 9 erg cm^{-2} (9×10^{-7} J cm^{-2}) while that for a metastable Cu–12.2 wt % Ge alloy is about 2 erg cm^{-2} (2×10^{-7} J cm^{-2}). There is also an indication that raising the temperature of a given composition will increase the SFE and promote narrower faults. This is consistent with the fact that higher temperatures promote randomness of solute distribution and increased stability of the fcc matrix with respect to the tendency for hcp phase formation. While solute diffusion is not considered an important condition for fault movement in the formation of a zeta plate, it is expected that the effectiveness of potential boundary dislocation nuclei will be influenced by the local solute content. In this way the operation of nucleating sites will be sensitive to the solution treatment, as reflected by the transformation curves in Fig. 1, which are displaced to longer times for higher solution temperatures.

The observations of the present work are consistent with an intergranular mechanism proposed by Horsewell *et al.* [11] for the fcc–hcp martensitic transformation. The change in stacking sequence from fcc to hcp is accomplished by the passage of Shockley partial dislocations over alternate close-packed planes in the cubic phase. High-angle grain boundaries were proposed as the major sources from which Shockley partials can be emitted in a regenerative manner to produce the groups of faults necessary for hcp platelet formation. This mechanism takes into account several important requirements for the fcc–hcp transformation:

1. The transforming partial dislocations must be produced in a regenerative manner to avoid the unlikely process of individual stacking-fault nucleation.
2. In order to avoid a total shape change it is necessary for the sum of the Burgers vectors to equal zero.
3. The transforming Shockley partials should be nucleated and regenerated almost as straight lines so that stacking fault expansion might occur spontaneously [11].

The emission of partial dislocations on alternate {1 1 1} planes of a given set depends on a reduction in free energy accompanying the production of hcp phase. For this process to occur it was proposed [11] that a Burgers vector equivalent to that of a matrix dislocation in one grain can be generated by the combination of appropriate grain-boundary dislocations. The emission of sets of three partials having Burgers vectors summing to zero avoids any shape change while preserving the orientation of the boundary plane and producing seven layers of hexagonal phase.

A similar concept was employed in developing models for martensite transformations in general [46] and the fcc–hcp transformation in particular by Olson and Cohen [13]. They concentrated on the energetics of the transformation by employing the concept of embryo formation due to a faulting process from "existing defects". For the fcc–hcp transformation their calculations indicate that a defect comprising four of five properly spaced lattice dislocations may satisfy the conditions for spontaneous transformation at the M_s temperature. The above models were developed primarily for martensitic transformations, but the observations of the present work clearly show that the thermal activation of the fcc–hcp transformation proceeds by a similar mechanism in Cu–Ge and Cu–Si alloys.

5. Summary and conclusions

1. Thin-foil studies show that the zeta phase, which initially forms during the initial stages of ageing, consists of groups of very thin platelets with thickness ranging from 5 to 30 nm. Continued ageing results in the formation of additional thin platelets, often in close proximity to existing platelets. The resulting morphology has been inappropriately termed "fault bundles" by other investigators. At optical magnifications, due to low resolution, the platelet clusters are in the form of thick hcp plates. The apparent thickening of these "plates" is due primarily to the formation of additional fine platelets to form bundles due to continuing nucleation.

2. Rapid quenching accelerates the rate of zeta formation by promoting the formation of additional thin platelets, rather than the thickening of existing platelets.

3. The transformation kinetics exhibit C-curve behaviour. The growth and "thickening" processes are not consistent with solute diffusion control, but are best described in terms of isothermal martensitic growth in which zeta phase formation is controlled by nucleation.

4. Grain boundaries and non-coherent twin boundaries are potential sites for nucleation. A grain-boundary fine structure, identified as a dislocation network, was observed and it is probable that such networks act as nuclei for the transformation.

5. The fcc–hcp transformation is viewed as depending on the activation of partial dislocations and may be viewed as operational in nature. It is proposed that once the nuclei are "triggered", growth occurs by the rapid movement of a "transformation interface" parallel to a given orientation of {1 1 1} planes. The interface is composed of a set of all three Shockley partial dislocations, which produce a net shear of zero. This is consistent with the observed orientation relationship and the completely coherent nature of the thin hcp platelets; it also obviates the formulation of a "thickening mechanism" which has been a problem in describing the growth of the hcp phase in the past. Some short-range solute diffusion is required for the hcp phase to achieve an equilibrium solute content, but is not rate-controlling with respect to platelet formation.

6. Decreasing the solution temperature increased the rates of zeta formation in Cu–Ge and kappa phase

in Cu–Si at a given ageing temperature, thereby indicating that solute distribution which is expected to influence the fault configuration is also an important parameter affecting nuclei operation.

Acknowledgements

The authors express thanks to the US Bureau of Mines, Albany, Oregon for assistance in preparing the alloys. This work was supported in part by a grant from the National Science Foundation, under Grant No. DMR-8411176.

References

1. W. HOFFMAN, J. ZIEGLER and H. HANEMANN, *Z. Metallkde* **42** (1952) 55.
2. G. A. DREYER and D. H. POLONIS, *Trans. TMS–AIME* **221** (1961) 1074.
3. P. S. KOTVAL and R. K. HONEYCOMBE, *Acta Metall.* **16** (1968) 597.
4. M. B. KASEN, PhD dissertation, University of Washington (1965).
5. S. D. DAHLGREN W. F. FLANAGAN and D. H. POLONIS, *Trans. TMS–AIME* **236** (1966) 1071.
6. P. S. KOTVAL, PhD thesis, University of Sheffield (England) (1965).
7. P. R. SWANN, "Electron Microscopy and Strength of Crystals" (Wiley, New York, 1965) p. 131.
8. K. R. KINSMAN, H. I. AARONSON and E. EICHEN, *Met. Trans.* **2** (1971) 1041.
9. M. B. KASEN, R. TAGGART and D. H. POLONIS, *Trans. Q. ASM* **60** (2) (1967) 144.
10. D. S. HALEY, R. TAGGART and D. H. POLONIS, *Scripta Metall.* **2** (1968) 585.
11. A. HORSEWELL, B. RALPH and P. R. HOWELL, *Phys. Status Solidi* **29** (1975) 587.
12. A. HORSEWELL, P. R. HOWELL and B. RALPH, "Grain Boundaries", Proceedings of Spring Residential Conference, Institution of Metallurgists Series 3 No. 5 (1976) p. B6.
13. G. B. OLSON and M. COHEN, *Met. Trans.* **7A** (1976) 1897.
14. *Idem, ibid.* **7A** (1976) 1915.
15. J. A. HREN and G. THOMAS, *Trans. TMS–AIME* **227** (1963) 308.
16. E. VOTAVA, *J. Inst. Metals* **90** (1961) 129.
17. J. M. HOWE, H. I. AARONSON and R. GRONSKY, *Acta Metall.* **33** (4) (1985) 639.
18. *Idem, ibid.* **33** (4) (1985) 649.
19. H. I. AARONSON, in "Decomposition of Austenite by Diffusional Processes", edited by V. F. Zackay and H. I. Aaronson (Interscience, New York, 1962) p. 397.
20. A. CLEMENT N. CLEMENT and O. COULOMB, *Phys. Status Solidi* **21** (1967) K97.
21. T. V. NORDSTROM and C. R. BARRETT, *Acta Metall.* **17** (1969) 139.
22. S. TAKEUCHI and T. HOMME, *Sci. Rep. Res. Inst., Tohoku Univ.* **9A** (1957) 492.
23. *Idem, ibid.* **9A** (1957) 508.
24. B. A. BILBY, *Phil. Mag.* **44** (1953) 782.
25. Z. S. BASINSKI and J. W. CHRISTIAN, *ibid.* **44** (1953) 791.
26. A. SEEGER, *Z. Metallkde* **44** (1953) 247.
27. *Idem, ibid.* **47** (1956) 653.
28. H. SUZUKI, *Sci. Rep. Res. Inst., Tohoku Univ.* **A4** (1952) 455.
29. P. B. HIRSCH, A. HOWIE, R. B. NICHOLSON, D. W. PASHLEY and M. J. WHELAN, "Electron Microscopy of Thin Crystals", (Butterworths, Washington, 1965).
30. A. KELLY and R. B. NICHOLSON, *Prog. Mater. Sci.* **10** (1963) 151.
31. J. D. EMBURY and R. B. NICHOLSON, *Acta Metall.* **13** (1965) 403.
32. P. J. MOROZ Jr, D. H. POLONIS and R. TAGGART, *Metallography* **2** (1969) 385.
33. P. J. MOROZ, R. TAGGART and D. H. POLONIS, *Mater. Sci. Eng.* **79** (1986) 201.
34. L. DELAEY, *Phys. Status Solidi* **25** (1968) 697.
35. G. THOMAS, W. L. BELL and H. M. OTTE, *ibid.* **12** (1965) 353.
36. R. GEVERS, J. VAN LANDUYT and S. AMELINCKX, *ibid.* **18** (1966) 343.
37. M. S. PATTERSON, *J. Appl. Phys.* **23** (1952) 805.
38. Y. ISHIDA and M. H. BROWN, *Acta Metall.* **15** (1967) 857.
39. Y. ISHIDA, T. HASEGAWA and F. NAGATA, *J. Appl. Phys.* **40** (1969) 2182.
40. B. LOBERG and H. NORDEN, *Acta Metall.* **21** (1973) 213.
41. R. R. CECH and J. H. HOLLOMAN, *Trans. TMS–AIME* **197** (1953) 615.
42. C. H. SHIH, B. L. AVERBACH and M. COHEN, *ibid.* **203** (1955) 183.
43. R. C. POND, "Grain Boundary Structure and Kinetics", ASM Materials Science Seminar, Milwaukee, 1979 (ASM, Metals Park, Ohio, 1980) p. 13.
44. K. H. G. ASHBEE and L. F. VASSAMILLET, *Mellon Inst. Rep.* (April 1966).
45. L. BROWN, *Phil. Mag.* **10** (1964) 441.
46. G. B. OLSON and M. COHEN, *Met. Trans.* **7A** (1976) 1905.

Received 3 March
and accepted 22 May 1986